Engineering Fluorescent Calcium Sensor Proteins for Imaging Neural Activity

Douglas S. Kim, PhD, Vivek Jayaraman, PhD,
Loren L. Looger, PhD, and Karel Svoboda, PhD

Janelia Research Campus
Howard Hughes Medical Institute
Ashburn, Virginia

SfN Society for Neuroscience

Introduction

Understanding neural circuit function requires making measurements of neural activity over many spatial and temporal scales. Calcium indicators have been especially useful for studying neuronal activity over these scales, especially for action potential (AP) detection. APs in most neurons are tightly coupled to large (20-fold) and rapid (rise time <1 ms) increases in intracellular free-calcium concentration. These calcium transients are proxies for the underlying electrical activity. They can be measured *in vitro* and *in vivo* as fluorescence changes of calcium indicators in neuronal somata (Stosiek et al., 2003; Reiff et al., 2005), dendrites (Svoboda et al., 1997; Seelig and Jayaraman, 2013), and axons (Cox et al., 2000; Petreanu et al., 2012). Calcium indicators are also useful in nonspiking, graded potential neurons (Haag and Borst, 2000; Seelig et al., 2010), although optimal indicator parameters may differ. Additionally, excitatory synaptic transmission is typically associated with large-amplitude (20- to 100-fold) increases in calcium concentration in small synaptic compartments (e.g., dendritic spines). These synaptic calcium transients can be used to quantify synaptic transmission *in vitro* (Yuste and Denk, 1995) and *in vivo* (Jia et al., 2010; Chen et al., 2013). Calcium imaging is useful for probing neural activity over physiological and behavioral timescales of milliseconds to months, and wide spatial ranges from micrometers to millimeters.

Genetically Encoded Calcium Indicators

Small-molecule calcium indicators (e.g., Fura2, Fluo4, OGB1) have excellent properties in terms of kinetics and fractional fluorescence change (Tsien, 1989). However, introducing these molecules into tissue is invasive and nonspecific. Loading the molecules is destructive and incompatible with long-term imaging. Fluorescent protein–based indicators can overcome these problems. Genetically encoded calcium indicators (GECIs) can be expressed in specific types of neurons using minimally invasive methods over chronic timescales (Mank et al., 2008; Tian et al., 2009; Lutcke et al., 2010; Akerboom et al., 2012; Chen et al., 2013). Additionally, protein indicators can be targeted to subcellular locations to report specific dynamic events of interest (Miyawaki et al., 1997; Mao et al., 2008). GECIs occupy a niche that complements single-unit electrophysiology. Although single-unit methods have better sensitivity and time resolution, through optimization, GECIs have been engineered that achieve signal-to-noise ratios (SNRs) that rival electrophysiological methods.

Multiple GECI types have been developed and improved over several development cycles. GCaMP and related sensors are based on circularly permuted green fluorescent protein (cpGFP) (Baird et al., 1999) linked to calmodulin (CaM) and the M13 peptide from myosin light-chain kinase (Nakai et al., 2001; Ohkura et al., 2005; Tallini et al., 2006; Tian et al., 2009; Zhao et al., 2011; Akerboom et al., 2012; Chen et al., 2013; Wu et al., 2013). For most GCaMP sensors, fluorescence intensity increases with elevated calcium. Ratiometric GCaMP variants have also been reported (Zhao et al., 2011). Cameleons consist of a pair of fluorescent proteins linked by CaM/M13 (Miyawaki et al., 1997; Nagai et al., 2004; Palmer et al., 2006). Calcium elevations cause a change in Förster resonance energy transfer. TN-XXL and its derivatives are similar to cameleons, but use the calcium-binding protein troponin to sense calcium (Mank et al., 2008; Thestrup et al., 2014).

Optimizing GCaMP, a GFP-based calcium indicator

GCaMP-type GECIs are widely used to provide a unique view into nervous system function. They have been used to measure the dynamics of large populations of neurons over times of weeks, even during learning (Tian et al., 2009; Akerboom et al., 2012; Huber et al., 2012; Chen et al., 2013). They can track activity in local and long-range axonal projections and provide information about the activity of neurons that are inaccessible to electrophysiological methods (Suzuki et al., 2003). Moreover, this GFP-based indicator has a large two-photon absorption cross-section at accessible excitation wavelengths for *in vivo* imaging through hundreds of microns of brain tissue.

GCaMP engineering has benefited from structure-based design (Fig. 1). GCaMP relies on a calcium-dependent interaction between CaM and the CaM-interacting M13 peptide, both fused to cpGFP. With cooperative calcium binding, the CaM/M13 interaction changes sensor conformation. This conformational shift modulates the environment of the cpGFP chromophore through formation of new domain interfaces, rearrangement of protein side chains, and reduction of solvent access to the chromophore. These rearrangements cause increased absorption and brightness with increasing calcium concentrations. The GCaMP crystal structure (Wang et al., 2008; Akerboom et al., 2009; Ding et al., 2014) revealed the importance of the CaM/cpGFP proto-interface in regulating chromophore function. Functional screening of GCaMP variants at the CaM/cpGFP interface and in other domains

NOTES

has produced indicators with improved fluorescence changes (Akerboom et al., 2012; Chen et al., 2013).

Sensitive GCaMP indicators

Recently, we developed the general-purpose GCaMP6 sensors for *in vivo* imaging of neuronal populations (Chen et al., 2013). We used a neuronal culture assay for GCaMP6 development (Wardill et al., 2013). The assay enabled rapid GECI characterization and optimization in the relevant cell type. Neurons have fast and small-amplitude calcium accumulations that are difficult to model in nonneuronal systems. Primary rat hippocampal cultures in multiwell plates were transduced with GECI variants and a nuclear fluorescent protein construct to control for expression level. APs were triggered using extracellular stimulation electrodes, while neurons were imaged using fluorescence microscopy. We imaged the fluorescence dynamics of multiple individual neurons responding to a variety of trains of APs. This neuronal culture assay allowed us to characterize large numbers of GECI variants under relevant conditions (Fig. 1).

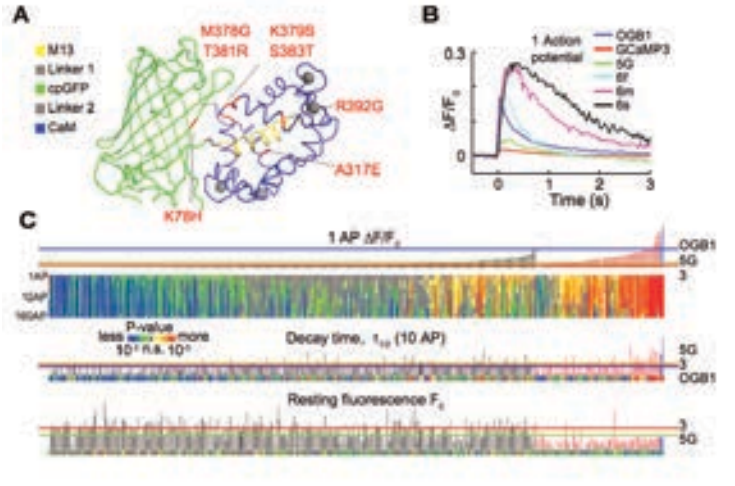

Figure 1. GCaMP6 engineering. ***A,*** GCaMP structure (Akerboom et al., 2009) and mutations in different GCaMP6 variants. M13 peptide (yellow), linker 1 (gray), cpGFP (green), linker 2 (gray), CaM (blue), and mutated positions found in GCaMP6 variants relative to GCaMP5G (red text). ***B,*** Responses averaged across multiple neurons and wells for GCaMP3, 5G, 6f, 6m, 6s, and OGB1-AM. Fluorescence changes in response to 1 AP. ***C,*** Screening results, 447 GCaMPs. Top, fluorescence change in response to 1 AP (vertical bars, $\Delta F/F_0$; green bar, OGB1-AM, left; black bars, single GCaMP mutations; red bars, combinatorial mutations; blue, GCaMP6 indicators) and significance values for 1, 2, 3, 5, 10, 20, 40, 80, and 160 AP stimuli compared with GCaMP3 (color plot). Middle, half decay time after 10 APs. Bottom, resting fluorescence, F_0 normalized to nuclear mCherry fluorescence. Red line, GCaMP3 level; green line, GCaMP5G level; blue line, OGB1-AM level. Figure adapted with permission from Chen et al. (2013), their Fig. 1*a–c*.

The GCaMP6 variants can reliably detect a single AP stimulus, with responses that equal or exceed the fluorescence response of the synthetic calcium dye OGB1 (Fig. 1). These highly sensitive GCaMP6 indicators differ in their speed. In cultured hippocampal neurons, GCaMP6s is slowest, with a decay time of 1.8 s ($\tau_{½}$ after 10 APs). GCaMP6m has faster kinetics while maintaining a high response. GCaMP6f is the fastest variant, with a 1 AP rise time-to-peak of ~50 ms and a decay time ($\tau_{½}$ after 1 AP) of ~140 ms. The GCaMP6 indicators have basal fluorescence levels (F_0) similar to those of GCaMP5G (Fig. 1*c*) (Akerboom et al., 2012).

Under favorable imaging conditions, these sensors detect single spikes in neuronal populations *in vivo* (Fig. 2) (Chen et al., 2013). GCaMP6s was expressed virally in the visual cortex of an anesthetized, adult mouse. Visual stimuli in the form of drifting gratings in different orientations of movement were shown to the mouse. The fraction of responding neurons using GCaMP6s exceeded the fraction detected with OGB1, likely because they detected weak responses missed by OGB1. In additional imaging experiments, responses from a layer 2/3 pyramidal neuron were simultaneously imaged using two-photon microscopy and recorded by patch electrode. The orientation-selective responses to single APs at the soma were reported with high sensitivity by GCaMP6s compared with those of previous indicators. GCaMP6f exhibited large $\Delta F/F_0$ (fluorescence change normalized by resting fluorescence) responses and a fast single-spike rise time-to-peak of ~50 ms. The high sensitivity of GCaMP6s enabled detection of even subthreshold dendritic spine activity in response to drifting gratings. Moreover, repeated imaging of the same neuron and processes over several weeks was conducted using GCaMP6s. The stability of the orientation tuning of dendritic spines was assessed with this high-sensitivity, genetically encoded sensor. GECIs with even higher sensitivity will allow larger populations of neurons to be imaged more rapidly and under more challenging conditions (e.g., imaging in awake and behaving animals).

Strategies for increasing GECI sensitivity

GECI sensitivity could be increased in several ways for different applications.

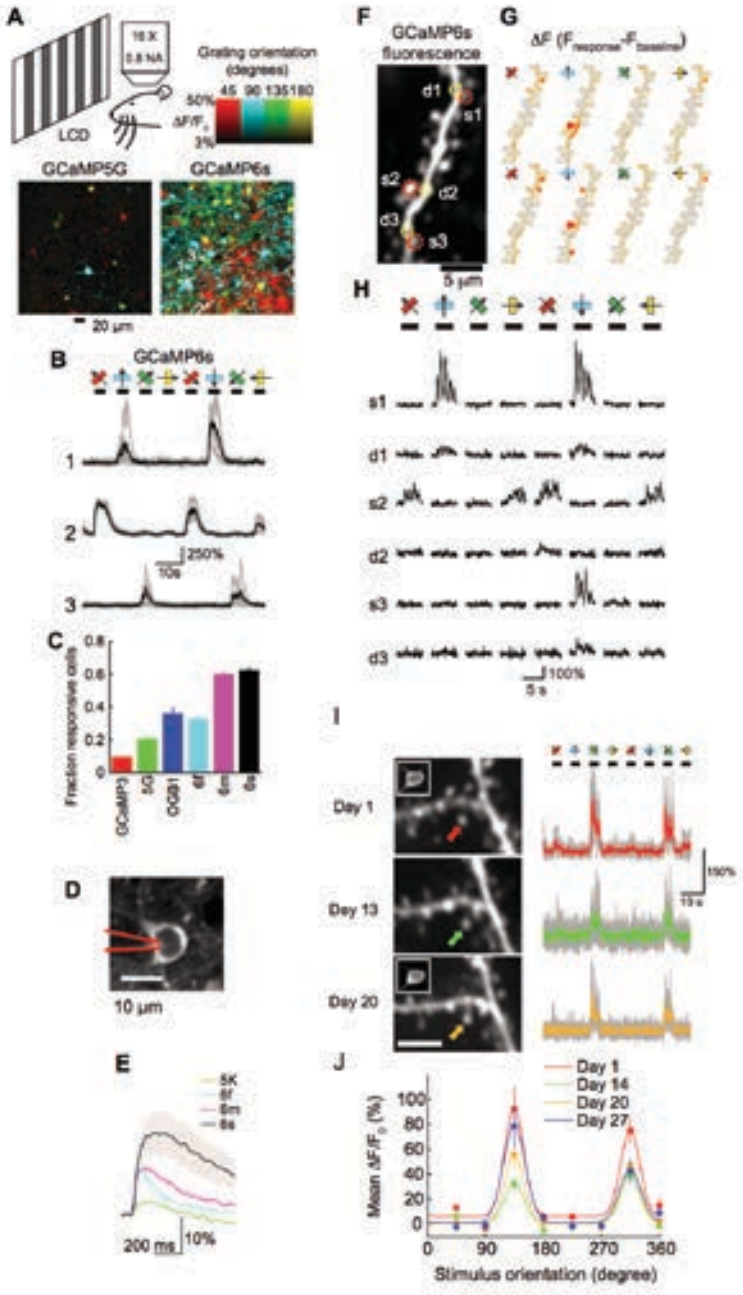

Figure 2. Imaging activity in neurons and dendritic spines in the mouse visual cortex. ***A,*** Top, schematic of the experiment. Bottom, field-of-view (FOV) showing neurons color-coded according to their preferred orientation (hue) and response amplitude (brightness) for GCaMP5G (left) and GCaMP6s (right). Scale bar, 20 μm. ***B,*** Example $\Delta F/F_0$ traces from 3 neurons expressing GCaMP6s. Single sweeps (gray) and averages of 5 sweeps (black) are overlaid. Directions of grating motion (8 directions) are shown above traces (arrows). ***C,*** The fraction of cells scored as responding to visual stimulation when loaded with different calcium indicators. Error bars correspond to SEM (n = 70, 39, 23, 38, 21, 34 FOVs) for GCaMP3, 5G, OGB1-AM, 6f, 6m, and 6s, respectively. ***D,*** Simultaneous fluorescence dynamics and spikes in a GCaMP6s-expressing neuron. GCaMP6s-expressing neuron with the recording pipette indicated schematically. Scale bar, 10 μm. ***E,*** Median fluorescence change in response to 1 AP for different calcium indicators. Shading corresponds to SEM, n = 9 (GCaMP5K; data from Akerboom et al., 2012), 11 (GCaMP6f), 10 (GCaMP6m), and 9 (GCaMP6s) cells. ***F,*** Image of a layer 2/3 dendritic branch expressing GCaMP6s. Regions of interest (ROIs) are indicated as dashed circles (red, spines; yellow, dendrites). ***G,*** Map of fluorescence change ($\Delta F = F_{response} - F_{baseline}$) in response to drifting gratings of 8 different orientations. ***H,*** Responses of dendritic spines (s1–s3) and neighboring dendritic shafts (d1–d3) to drifting gratings with different orientations (corresponding to ROIs indicated in ***F***). ***I,*** Left, the same GCaMP6s-labeled spine imaged over weeks. Right, fluorescence responses to oriented drifting gratings. Insets, parent soma of imaged spines. ***J,*** Orientation selectivity of single spines measured over time (same as ***I***). Figure adapted with permission from Chen et al. (2013), their Figs. 2–4.

NOTES

The high sensitivity of GCaMP6s and 6f was achieved by both increasing the dynamic range (ratio of calcium-saturated fluorescence to calcium-free fluorescence; F_{sat}/F_{apo}) and increasing calcium affinity of the sensor compared with previous GCaMP variants. The high affinity leads to saturation of these sensors at modest activity levels, making them unsuitable for monitoring activity patterns in neurons with high spike rates (>100 Hz). The saturation of GCaMP6 variants was evident in the high-frequency motor neurons of *Drosophila* larvae (Fig. 3). For example, GCaMP6m accurately tracked individual spikes in motor neuron boutons at the larval neuromuscular junction when stimulated at low frequencies (1–5 Hz), but the fluorescence responses reached a plateau at higher frequencies (40–160 Hz). Engineering GECIs with lower affinity will aid in tracking high-frequency activity and graded potential neuronal activity. In addition, GCaMP is CaM-based and contains four calcium-binding domains that cooperate in binding calcium. Reducing the binding cooperativity could increase the linear range for detecting calcium changes.

Intracellular calcium is highly buffered by endogenous proteins in some neurons and can make imaging with calcium sensors challenging. Parvalbumin-positive interneurons exhibit relatively low fluorescence responses when loaded with OGB1 compared with excitatory neurons (Kerlin et al., 2010). In contrast to the above approach, engineering GECIs with very high affinity could be particular useful for increasing sensitivity in these neuronal subtypes. Ultrasensitive YC-nano indicators with very high calcium affinity (K_d~15 nM) have been reported (Horikawa et al., 2010).

Additional strategies for increasing GECI sensitivity can be explored. The SNR of GECIs can also be improved by minimizing the resting fluorescence without reducing the peak fluorescence. Lowering the background fluorescence from inactive neurons and processes while maintaining peak fluorescence will serve to increase SNR, especially

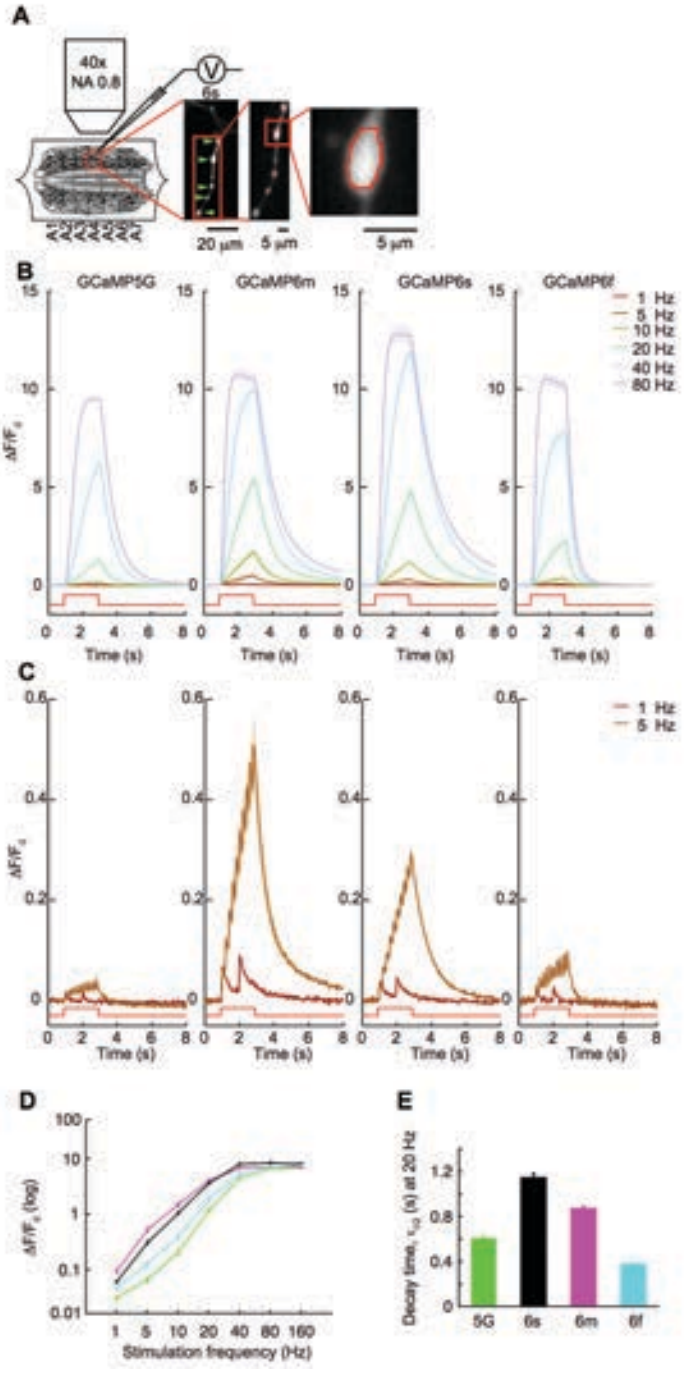

Figure 3. Fluorescence activity imaging in ***Drosophila*** larval neuromuscular junction boutons. ***A,*** Schematic of larval NMJ stimulation and imaging, epifluorescence (green arrow heads), and high magnification $\Delta F/F_0$ images of Type 1b boutons from muscle 13 (segments A3–A5). ***B,*** Average $\Delta F/F_0$ (± SEM) traces recorded after 1, 5, 10, 20, 40, and 80 Hz (green, cyan, magenta, black; n = 10, 12, 14, 12 FOVs, respectively) stimulus for 2 s (red) for GCaMP5G, 6m, 6s, and 6f. ***C,*** Average $\Delta F/F_0$ traces recorded after 1 and 5 Hz stimulus for 2 s. ***D,*** Average peak $\Delta F/F_0$ from 1 to 160 Hz. ***E,*** Average half decay time after 20 Hz stimulation for 2 s. Figure adapted with permission from Chen et al. (2013), their Supplementary Fig. 3.

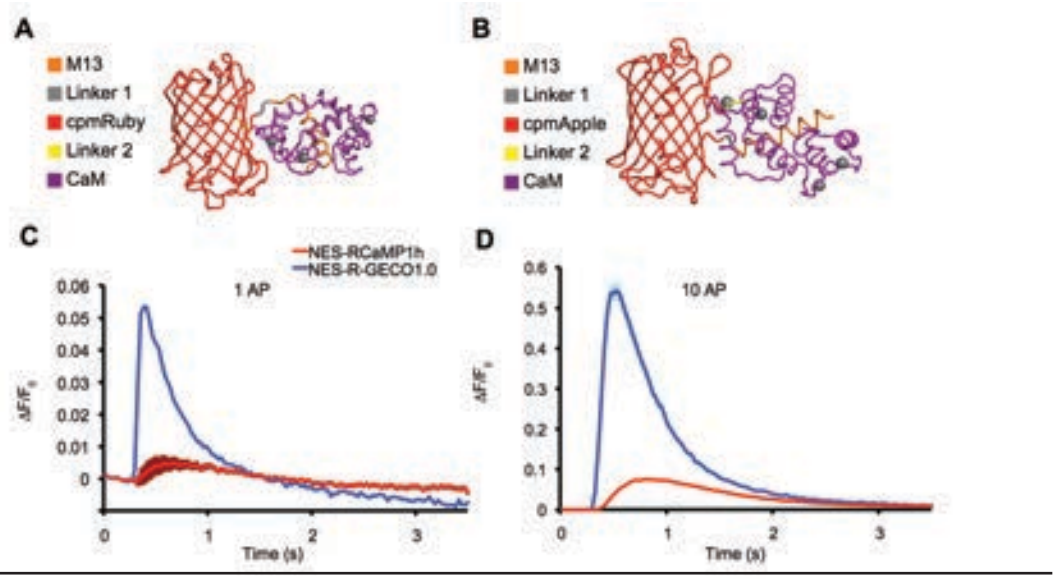

Figure 4. Red GECIs and their performance in cultured neurons. ***A,*** RCaMP1 structure including cpmRuby fluorescent protein (red), M13 peptide (orange), linker 1 (gray), CaM (purple), and linker 2 (yellow) (Akerboom et al., 2012). ***B,*** R-GECO1.0 structure including cpmApple fluorescent protein (red) (Akerboom et al., 2012). ***C,*** Averaged fluorescence response of neuronal cell bodies in culture to 1 AP stimulus. Nuclear export signal (NES)–tagged RCaMP1h (red), NES-R-GECO1.0 (blue). ***D,*** 10 AP stimulus.

with epifluorescence imaging of large populations of neurons. In the past, GCaMP variants with appreciable resting fluorescence were produced to enable structural imaging and identification of GECI-expressing neurons. However, transgenic animals now allow imaging in a background in which neurons, nuclei, or other structures of interest are labeled with a red fluorescent protein (RFP), obviating the need for substantial GCaMP resting fluorescence. Reducing resting fluorescence even by a factor of two while maintaining high peak fluorescence levels will have a substantial impact on SNR, increasing the yield in cellular imaging experiments by several-fold. In this manner, the scale of monitored neurons could be increased.

Fast GCaMP sensors

Existing GECIs are relatively slow compared with the speed of APs in part because of sensor protein dynamics. Calcium binds and unbinds cooperatively to the CaM EF-hand domains 100- to 1000-fold faster than the onset and offset of GCaMP fluorescence (Faas et al., 2011). GCaMP response kinetics have been improved, particularly with GCaMP6f, which has relatively fast rise (~50 ms, 1 AP τ_{peak}) and decay (~140 ms, 1 AP $\tau_{1/2}$) times while maintaining OGB1-like SNR (Chen et al., 2013). GCaMP6f incorporates a mutation that is predicted to disrupt the M13/CaM interaction (A317E, Fig. 1). The M13/CaM interaction is likely a slow step downstream of calcium binding that affects the rate of fluorescence onset (Sun et al., 2013). The M13/CaM interaction affects calcium binding and unbinding, and thus, changing this interaction can also affect fluorescence offset rate.

GCaMP6f reports AP timing in neurons better than other GECIs. For example, GCaMP6f accurately tracked spiking at moderate frequencies (20 Hz) better than GCaMP6s at the *Drosophila* neuromuscular junction (NMJ) (Fig. 3). The decay time was inversely related to calcium K_d. GCaMP6f (K_d~375 nM) is also faster than GCaMP6s (K_d~144 nM). Faster variants can be engineered without altering affinity (Sun et al., 2013). In the future, fast GECIs with appropriate affinity, high SNR, and broad dynamic range will be most useful.

Optimizing red GECIs, RCaMP, and R-GECO

GECIs based on red-shifted fluorescent proteins have been made, including RCaMP, R-GECO, O-GECO, and CAR-GECO (Fig. 4) (Zhao et al., 2011; Akerboom et al., 2013; Wu et al., 2013). Red indicators are of particular interest for several reasons. First, longer wavelength excitation light penetrates deeper into tissue. In addition, red fluorescence is absorbed much less than green fluorescence, especially in mammalian tissue, giving red fluorophores a competitive advantage for *in vivo* imaging. Red GECIs therefore enable deeper and less invasive imaging than green GECIs. Second, combinations of red and green GECIs promise simultaneous imaging of multiple distinct neural structures (Li et al., 2013). Third, red GECIs are more easily combined with channelrhodopsin-2 (ChR2)–based manipulations

NOTES

of neural circuits because their excitation spectra are separated. Finally, many transgenic animals with green fluorescence have been created; red GECIs can be used in these animals. Optimized red GECIs will thus be useful individually or in combination with green GECIs.

Multicolor neuronal imaging ideally employs sensors with matched performance in each channel. The first-generation red GECIs, RCaMP1h and R-GECO1.0, underperformed green GECIs, such as GCaMP6s and GCaMP6f, in several ways (Figs. 1, 4). Both had inferior maximal dynamic range in solution measurements and responses after 160 AP stimulation at 83 Hz (Table 1). The red GECIs also had lower apparent calcium affinity compared with the green GECIs. The 1 AP fluorescence response was worse than that of GCaMP sensors. The red sensors were also slower than GCaMP6f. In general, RCaMP1h and R-GECO1.0 were less sensitive than GCaMP6s.

Newer red GECIs are improved and have begun to approach GCaMP6 sensitivity levels (Ohkura et al., 2012; Wu et al., 2013). R-GECO1.2 has improved dynamic range ($F_{calcium\text{-}saturated}/F_{calcium\text{-}free}$ = 33) compared with R-GECO1.0 but has lower affinity (Kd~1200 nM) than GCaMP6 variants (Wu et al., 2013). The orange GECI, O-GECO1 (based on mOrange) has excellent dynamic range ($F_{calcium\text{-}saturated}/F_{calcium\text{-}free}$ = 14) but lower affinity (K_d~1500 nM). Further optimization of these and other red GECIs will enable multicolor imaging with GCaMP6. Improved red GECIs will also enhance single red-channel imaging.

Red GECIs have been more challenging to engineer because of photophysical limitations of RFPs related to brightness and bleaching. Ideally, the brightness of the calcium-bound state would be maximized. Dim GECIs have lower SNR and require more laser power. Among red GECIs, RCaMP is the brightest molecule (extinction coefficient*quantum yield = 33 mM^{-1} cm^{-1}) relative to GCaMP6s (42 mM^{-1} cm^{-1}) (Table 2). The calcium-saturated brightnesses of R-GECO1.0, R-GECO1.2, O-GECO1, and CAR-GECO1 are all less than half that of RCaMP1h.

Under two-photon excitation, RFPs and red GECIs tend to bleach rapidly and/or show reversible dark states. The peak brightness per molecule (an experimental quantity proportional to quantum efficiency and inversely related to bleaching rate) (Mutze et al., 2012) is substantially smaller for R-GECO1.0 and RCaMP1h compared with GCaMP (~33% and ~50%, respectively) (Akerboom et al., 2013). In addition, R-GECO1.0 is transiently induced to become red fluorescent after exposure to blue light, which makes it incompatible with the action spectrum of ChR2 (Akerboom et al., 2013; Wu et al., 2013). Engineering to increase chromophore brightness, stability, and spectral purity could improve red GECIs substantially.

Conclusion

For more than 15 years, fluorescent proteins have been engineered to report neural activity. Although GECIs are now routinely used to image neuronal activity *in vivo*, they still have limitations. Quantitative testing of GECIs in neurons has accelerated calcium-sensor optimization in terms of sensitivity, speed, and dynamic range. GECI photostability and expression systems for *in vivo* imaging await further improvement. Better indicators will enable the dissection of neural circuits through the correlation of specific neuronal activity with behavior at higher resolution and over wider populations of neurons. Activity indicators for other neuronal state variables

Table 1. GECI sensitivity and kinetic parameters (Akerboom et al., 2012; Chen et al., 2013)

GECI	$F_{calcium\text{-}saturated}/F_{calcium\text{-}free}$	$\Delta F/F_0$ (160 AP)	K_d(nM)	$\Delta F/F_0$ (1 AP)	Decay $\tau_{½}$ (10 AP) (s)
RCaMP1h	11	3	1300	0.02	1.8
R-GECO1.0	16	8	449	0.08	0.8
GCaMP6s	63	17	144	0.23	1.8
GCaMP6f	52	13	375	0.19	0.4

Table 2. GECI brightness measured in solution (Akerboom et al., 2012; Chen et al., 2013)

GECI	Brightness (extinction coefficient*quantum yield, mM^{-1} cm^{-1})
GCaMP6s	42
RCaMP1h	33
R-GECO1.0	11
R-GECO1.2	15
O-GECO1	14
CAR-GECO1	8

(e.g., membrane voltage) and light-gated effectors that alter activity will also be critical for *in vivo*, light-based neurophysiology.

Acknowledgments

The Genetically-Encoded Neuronal Indicator and Effector (GENIE) Project at the Janelia Research Campus is funded by the Howard Hughes Medical Institute. Primary data included here were produced by past and present members and collaborators with the project, including Tsai-Wen Chen, Trevor J. Wardill, Yi Sun, Hod Dana, Jasper Akerboom, Stefan R. Pulver, Ronak Patel, John J. Macklin, Eric R. Schreiter, Benjamin F. Fosque, and Douglas S. Kim. Technical expertise was provided by Jeremy P. Hasseman, Getahun Tsegaye, Reza Behnam, Brenda C. Shields, Zijuan Ma, Amy Hu, Melissa Ramirez, and Kimberly Ritola. We thank other collaborators including Sabine L. Renninger, Michael B. Orger, Amy Baohan, Lin Tian, and Bruce E. Kimmel. The project was supervised by Douglas S. Kim, Rex A. Kerr, Vivek Jayaraman, Loren L. Looger, and Karel Svoboda. We thank our many colleagues at Janelia and elsewhere who have contributed to this work through helpful discussions and sharing reagents. Parts of this chapter were adapted from Akerboom et al., 2013; Chen et al., 2013; and Wardill et al., 2013.

References

Akerboom J, Rivera JD, Guilbe MM, Malave EC, Hernandez HH, Tian L, Hires SA, Marvin JS, Looger LL, Schreiter ER (2009) Crystal structures of the GCaMP calcium sensor reveal the mechanism of fluorescence signal change and aid rational design. J Biol Chem 284:6455–6464.

Akerboom J, Chen TW, Wardill TJ, Tian L, Marvin JS, Mutlu S, Calderón NC, Esposti F, Borghuis BG, Sun XR, Gordus A, Orger MB, Portugues R, Engert F, Macklin JJ, Filosa A, Aggarwal A, Kerr RA, Takagi R, Kracun S, et al. (2012) Optimization of a GCaMP Calcium Indicator for Neural Activity Imaging. J Neurosci 32:13819–13840.

Akerboom J, Carreras Calderón N, Tian L, Wabnig S, Prigge M, Tolö J, Gordus A, Orger MB, Severi KE, Macklin JJ, Patel R, Pulver SR, Wardill TJ, Fischer E, Schüler C, Chen TW, Sarkisyan KS, Marvin JS, Bargmann CI, Kim DS, et al. (2013) Genetically encoded calcium indicators for multi-color neural activity imaging and combination with optogenetics. Front Mol Neurosci 6:2.

Baird GS, Zacharias DA, Tsien RY (1999) Circular permutation and receptor insertion within green fluorescent proteins. Proc Natl Acad Sci USA 96:11241–11246.

Chen TW, Wardill TJ, Sun Y, Pulver SR, Renninger SL, Baohan A, Schreiter ER, Kerr RA, Orger MB, Jayaraman V, Looger LL, Svoboda K, Kim DS (2013) Ultrasensitive fluorescent proteins for imaging neuronal activity. Nature 499:295–300.

Cox CL, Denk W, Tank DW, Svoboda K (2000) Action potentials reliably invade axonal arbors of rat neocortical neurons. Proc Natl Acad Sci USA 97:9724–9728.

Ding J, Luo AF, Hu L, Wang D, Shao F (2014) Structural basis of the ultrasensitive calcium indicator GCaMP6. Science China Life Sci 57:269–274.

Faas GC, Raghavachari S, Lisman JE, Mody I (2011) Calmodulin as a direct detector of Ca^{2+} signals. Nat Neurosci 14:301–304.

Haag J, Borst A (2000) Spatial distribution and characteristics of voltage-gated calcium signals within visual interneurons. J Neurophysiol 83:1039–1051.

Horikawa K, Yamada Y, Matsuda T, Kobayashi K, Hashimoto M, Matsu-ura T, Miyawaki A, Michikawa T, Mikoshiba K, Nagai T (2010) Spontaneous network activity visualized by ultrasensitive Ca(2+) indicators, yellow Cameleon-Nano. Nat Methods 7:729–732.

Huber D, Gutnisky DA, Peron S, O'Connor DH, Wiegert JS, Tian L, Oertner TG, Looger LL, Svoboda K (2012) Multiple dynamic representations in the motor cortex during sensorimotor learning. Nature 484:473–478.

Jia H, Rochefort NL, Chen X, Konnerth A (2010) Dendritic organization of sensory input to cortical neurons *in vivo*. Nature 464:1307–1312.

Kerlin AM, Andermann ML, Berezovskii VK, Reid RC (2010) Broadly tuned response properties of diverse inhibitory neuron subtypes in mouse visual cortex. Neuron 67:858–871.

Li H, Li Y, Lei Z, Wang K, Guo A (2013) Transformation of odor selectivity from projection neurons to single mushroom body neurons mapped with dual-color calcium imaging. Proc Natl Acad Sci USA 110:12084–12089.

NOTES

Lutcke H, Murayama M, Hahn T, Margolis DJ, Astori S, Zum Alten Borgloh SM, Gobel W, Yang Y, Tang W, Kugler S, Sprengel R, Nagai T, Miyawaki A, Larkum ME, Helmchen F, Hasan MT (2010) Optical recording of neuronal activity with a genetically-encoded calcium indicator in anesthetized and freely moving mice. Front Neural Circ 4:9.

Mank M, Santos AF, Direnberger S, Mrsic-Flogel TD, Hofer SB, Stein V, Hendel T, Reiff DF, Levelt C, Borst A, Bonhoeffer T, Hubener M, Griesbeck O (2008) A genetically encoded calcium indicator for chronic *in vivo* two-photon imaging. Nat Methods 5:805–811.

Mao T, O'Connor DH, Scheuss V, Nakai J, Svoboda K (2008) Characterization and subcellular targeting of GCaMP-type genetically-encoded calcium indicators. PloS One 3:e1796.

Miyawaki A, Llopis J, Heim R, McCaffery JM, Adams JA, Ikura M, Tsien RY (1997) Fluorescent indicators for Ca^{2+} based on green fluorescent proteins and calmodulin. Nature 388:882–887.

Mutze J, Iyer V, Macklin JJ, Colonell J, Karsh B, Petrasek Z, Schwille P, Looger LL, Lavis LD, Harris TD (2012) Excitation spectra and brightness optimization of two-photon excited probes. Biophys J 102:934–944.

Nagai T, Yamada S, Tominaga T, Ichikawa M, Miyawaki A (2004) Expanded dynamic range of fluorescent indicators for Ca^{2+} by circularly permuted yellow fluorescent proteins. Proc Natl Acad Sci USA 101:10554–10559.

Nakai J, Ohkura M, Imoto K (2001) A high signal-to-noise Ca(2+) probe composed of a single green fluorescent protein. Nat Biotechnol 19:137–141.

Ohkura M, Matsuzaki M, Kasai H, Imoto K, Nakai J (2005) Genetically encoded bright Ca^{2+} probe applicable for dynamic Ca^{2+} imaging of dendritic spines. Anal Chem 77:5861–5869.

Ohkura M, Sasaki T, Sadakari J, Gengyo-Ando K, Kagawa-Nagamura Y, Kobayashi C, Ikegaya Y, Nakai J (2012) Genetically encoded green fluorescent Ca^{2+} indicators with improved detectability for neuronal Ca^{2+} signals. PloS one 7:e51286.

Palmer AE, Giacomello M, Kortemme T, Hires SA, Lev-Ram V, Baker D, Tsien RY (2006) Ca^{2+} indicators based on computationally redesigned calmodulin-peptide pairs. Chem Biol 13:521–530.

Petreanu L, Gutnisky DA, Huber D, Xu NL, O'Connor DH, Tian L, Looger L, Svoboda K (2012) Activity in motor-sensory projections reveals distributed coding in somatosensation. Nature 489:299–303.

Reiff DF, Ihring A, Guerrero G, Isacoff EY, Joesch M, Nakai J, Borst A (2005) *In vivo* performance of genetically encoded indicators of neural activity in flies. J Neurosci 25:4766–4778.

Seelig JD, Jayaraman V (2013) Feature detection and orientation tuning in the *Drosophila* central complex. Nature 503:262–266.

Seelig JD, Chiappe ME, Lott GK, Dutta A, Osborne JE, Reiser MB, Jayaraman V (2010) Two-photon calcium imaging from head-fixed *Drosophila* during optomotor walking behavior. Nat Methods 7:535–540.

Stosiek C, Garaschuk O, Holthoff K, Konnerth A (2003) *In vivo* two-photon calcium imaging of neuronal networks. Proc Natl Acad Sci USA 100:7319–7324.

Sun XR, Badura A, Pacheco DA, Lynch LA, Schneider ER, Taylor MP, Hogue IB, Enquist LW, Murthy M, Wang SSH (2013) Fast GCaMPs for improved tracking of neuronal activity. Nat Commun 4:2170.

Suzuki H, Kerr R, Bianchi L, Frokjaer-Jensen C, Slone D, Xue J, Gerstbrein B, Driscoll M, Schafer WR (2003) *In vivo* imaging of *C. elegans* mechanosensory neurons demonstrates a specific role for the MEC-4 channel in the process of gentle touch sensation. Neuron 39:1005–1017.

Svoboda K, Denk W, Kleinfeld D, Tank DW (1997) *In vivo* dendritic calcium dynamics in neocortical pyramidal neurons. Nature 385:161–165.

Tallini YN, Ohkura M, Choi BR, Ji G, Imoto K, Doran R, Lee J, Plan P, Wilson J, Xin HB, Sanbe A, Gulick J, Mathai J, Robbins J, Salama G, Nakai J, Kotlikoff MI (2006) Imaging cellular signals in the heart *in vivo*: Cardiac expression of the high-signal Ca^{2+} indicator GCaMP2. Proc Natl Acad Sci USA 103:4753–4758.

Thestrup T, Litzlbauer J, Bartholomaus I, Mues M, Russo L, Dana H, Kovalchuk Y, Liang Y, Kalamakis G, Laukat Y, Becker S, Witte G, Geiger A, Allen T, Rome LC, Chen TW, Kim DS, Garaschuk O, Griesinger C, Griesbeck O (2014) Optimized ratiometric calcium sensors for functional *in vivo* imaging of neurons and T lymphocytes. Nat Methods 11:175–182.

Tian L, Hires SA, Mao T, Huber D, Chiappe ME, Chalasani SH, Petreanu L, Akerboom J, McKinney SA, Schreiter ER, Bargmann CI, Jayaraman V, Svoboda K, Looger LL (2009) Imaging neural activity in worms, flies and mice with improved GCaMP calcium indicators. Nat Methods 6:875–881.

Tsien RY (1989) Fluorescent probes of cell signaling. Annu Rev Neurosci 12:227–253.

Wang Q, Shui B, Kotlikoff MI, Sondermann H (2008) Structural basis for calcium sensing by GCaMP2. Structure 16:1817–1827.

Wardill TJ, Chen TW, Schreiter ER, Hasseman JP, Tsegaye G, Fosque BF, Behnam R, Shields BC, Ramirez M, Kimmel BE, Kerr RA, Jayaraman V, Looger LL, Svoboda K, Kim DS (2013) A neuron-based screening platform for optimizing genetically-encoded calcium indicators. PloS one 8:e77728.

Wu J, Liu L, Matsuda T, Zhao Y, Rebane A, Drobizhev M, Chang YF, Araki S, Arai Y, March K, Hughes TE, Sagou K, Miyata T, Nagai T, Li WH, Campbell RE (2013) Improved orange and red Ca(2)+/– indicators and photophysical considerations for optogenetic applications. ACS Chem Neurosci 4:963–972.

Yuste R, Denk W (1995) Dendritic spines as basic functional units of neuronal integration. Nature 375:682–684.

Zhao Y, Araki S, Wu J, Teramoto T, Chang YF, Nakano M, Abdelfattah AS, Fujiwara M, Ishihara T, Nagai T, Campbell RE (2011) An expanded palette of genetically encoded Ca(2) indicators. Science 333:1888–1891.